Microstructural evolution, recovery and recrystallization kinetics of isothermally annealed ultra low carbon steel

Materials Research Express

PAPER

Microstructural evolution, recovery and recrystallization kinetics of isothermally annealed ultra low carbon steel

Siuli Dutta[1,2], Ashis K Panda[1], Amitava Mitra[1], Subrata Chatterjee[2] and Rajat K Roy[1]

[1] NDE and Magnetic Materials, AMP Division, CSIR-National Metallurgical Laboratory, Jamshedpur-831007, India
[2] School of Materials Science and Engineering, IIEST, Shibpur, Howrah-731003, India

E-mail: rajat@nmlindia.org **and** rajatroy.k@gmail.com

Keywords: annealing, ultra low carbon steel, coercivity, hardness, recrystallization

OPEN ACCESS

RECEIVED
14 October 2019

REVISED
5 December 2019

ACCEPTED FOR PUBLICATION
24 December 2019

PUBLISHED
13 January 2020

Abstract

The recovery and recrystallization kinetics of 80% cold rolled ultra low carbon steel are investigated during isothermally annealing for temperature ranges 350–640 °C as a function of different annealing time. The recovery is assessed by magnetic coercivity (Hc), while the recrystallization is determined by mechanical hardness. At low temperature (350 to 520 °C) annealing, recovery dominates for long time (~12 000 s), while the annealing at 550 °C/ 900s and 580 °C/ 300s causes the recrystallized nuclei formation . The recovery kinetics is introduced by differential rate equation, explaining the reduction in coercivity with the recovery progress and the variation of an activation energy from 41–113 kJ mol^{-1}. The recrystallization kinetics is found faster at high annealing temperature 640 °C than 550 and 580 °C based on hardness measurement, justifying by apparent activation energy within 114–190 kJ mol^{-1}. Furthermore, the recovery and recrystallization rate increase with different annealing time, consistent to the change of microstructures and grain boundary characteristics evaluated by the orientation imaging microscopy (OIM) of electron backscattered diffraction (EBSD).

1. Introduction

The annealing treatment of low carbon steel results in the formation of substructure and new strain free grains with low dislocation density by recovery and recrystallization stages, respectively. The former stage relates to the annihilation of point defects and rearrangement of dislocations, while the latter one leads to movement of high angle boundaries through the growing of strain free grains [1]. In recovery, the observation of microstructural changes is insignificant at low magnification of optical and scanning electron microscopy (SEM). The high magnification analysis by transmission electron microscopy (TEM) can only provide the information of dislocation density to recognize recovery stage. Alternatively, various methods have been introduced for indirect monitoring of recovery and recrystallization process, correlating to the change in the bulk properties, such as tensile strength [2], hardness [3], phase intensity [4], resistivity [5], thermal enthalpy [6], magnetic coercive field [7, 8] etc. Amongst these techniques, the magnetic properties are determined on the non-destructive principle with a short response of time, leading to their applications for material evaluation at remote places during material processing as well as structural health monitoring [9]. The magnetic coercive field measurement has been found as an effective technique for the evaluation of creep [10], tempering [11, 12], residual stress [13], tensile deformation [14], recovery and recrystallization behaviors for various types of steels [15]. A good correlation is established between magnetic parameters such as coercivity, permeability, hysteresis-loss, flux density remanance with microstructure and mechanical properties of steels [16–18]. Kikuchi *et al* explained recovery and recrystallization behaviors of isothermal annealed low carbon steels by coercivity and hardness reductions, respectively [19]. A recent research on recovery and recrystallization kinetics for extra low carbon and micro alloyed steels also described a good correlation between coercivity (Hc) and mechanical hardness of steel. The coercivity is found a proportional relation to the square root of dislocation density and an inverse relation to recrystallized grain size [20, 21]. Accordingly, the coercive field (Hc) is clarified as an important parameter for the evaluation of recovery and recrystallization behavior of cold rolled steels through magnetic

softening [22]. The material softening is a thermally activated process in which material composition, annealing temperature and time are controlling factors. The softening kinetics determination is important to optimize alloy composition and processing conditions for controlling final steel properties. Several investigations have been reported to explain recovery and recrystallization kinetics using an empirical relation of logarithmic or exponential time dependence at post isothermal annealing treatment [4, 23–25]. Moreover, the recrystallization kinetics is described in terms of Johnson–Mehl-Avrami-Kolmagorov (JMAK) equation [26]. The recovery kinetics commonly controlled by thermally activated glide or the cross-slip of dislocations, driving to an activation energy Q, as a decreasing function of the internal stress [1, 27]. Rabbe *et al* have been explained the isothermal annealing effect on the recovery and recrystallization, and a corresponding change in microstructure fractions measured on the basis of EBSD method analysis [28]. The EBSD grain boundary map is able to define the change in grain boundary fractions during recovery and recrystallization. In this mapping, the recovery explains grain boundary misorientation within low angle at two ranges 2–5° and 5–15°, while the recrystallization represents angular misorientation above 15°. In addition, the resolved stored energy distribution after cold deformation as well as the changes in this distribution through subsequent annealing is conducted based on EBSD KAM analysis [29]. The purpose of present research work is to investigate the recovery and recrystallization kinetics of the cold rolled ultra low carbon steels at different annealed conditions through magnetic and mechanical softening behavior.

2. Experimentation

A hot deformed industrially processed steel sheet (5 mm thickness) is uniformly reduced to the final thickness of 2 mm by 80% deformation in a laboratory cold rolling (total 8 no. rolling passes) at room temperature. The chemical composition of steel sheet was Fe-99.61 C- 0.003 N-0.007 S-0.01 Ti-0.0025 Mn-0.195 Si -0.002 Cr-0.023 P-0.009 Cu- 0.006 (in wt%) . The test specimens were cut in the dimension of length and width of (100×40) mm^2, parallel to the rolling direction (RD). The cold rolled specimen was isothermally annealed at temperatures of 350, 400, 520, 550, 580 and 640 °C under the inert (argon gas) atmosphere in a tube furnace at a heating rate of 15 °C s^{-1} for different holding time ranging 0–12 000 s(~4.16 h). Magnetic properties of cold rolled and annealed specimens were measured by an indigenously developed electromagnetic sensing device, known as Magstar [30]. Measurements were carried out at each annealing condition (along the longitudinal directions RD) with an applied sinusoidal field of strength 120 kA m^{-1} and frequency of 0.05 Hz for magnetic hysteresis loop (MHL) measurement. The mechanical hardness of sheet surface (along RD) was measured by a Vickers hardness tester (ECONOMET VH-50MD) with an average value of five different points at a load of 30 kgf for 15 s. The microscopy specimens of rectangular size (12×10 mm^2) were cut along sheet surface in rolling direction (RD), and followed by grinding using different grades of SiC emery papers. The ground specimens were finally finished by coarse and fine polishing through alumina and silica colloidal solution, respectively. The mirror-like samples were observed by a FEG-SEM of FEI (Model: FEI-430 NOVA NANO) under an Electron Back Scattered Diffraction (EBSD) with an accelerating voltage of 20 KV, step size of 0.5 μm and selected scanned area of 300 μm $\times$ 250 μm. A TSL–OIM data analysis software was used to determine the quantification of annealed microstructures. The lattice imperfection stored energy spreading in cold rolled and annealed samples is signified by EBSD Kernel Average Misorientation (KAM) map.

3. Results and discussion

3.1. Microstructural evolution

The microstructure evoluation of annealed specimens is carrired out by orientation imaging map (OIM), explaining through inverse pole figure (IPF), grain boundary map and KAM map. In the present investigation, the kernel average misorientation (KAM) maps deliberate first neighbor with a threshold angle of 5°, and the significance of these color coded maps is presented at the bottom of the figure. The different colors of IPF map explain the grain orientation, e.g., red for ⟨001⟩, blue for ⟨111⟩, green for ⟨101⟩. The low temperature (400 °C) annealing (figure 1(a)), shows maximum grain orientation of ⟨111⟩ similar to reported cold deformed alloy [22]. With the increasing annealing temperature at 520 °C, the ferrite grains are mostly orientated towards the ⟨001⟩ and ⟨111⟩//ND during recovery stage (figure 1(b)), leading to subgrain fractions. The post annealing at 580 °C results in the onset of strain free grains with ⟨111⟩ orientation component and high angle boundaries in the ferrite deformed matrices, represented by the yellow arrows in figure 1(c). This observation is steady with the ideal concept of nucleation, i.e., related to the strain free grain formation at subgrain structure [31]. The partial clusters of recrystallized grains with random orientation are observed in the deformed matrix after annealing at 640 °C for 300 s (figure 1(d)). Finally, the complete equiaxed ferrite grains with an average size of 14 μm are found in the sample annealed at 640 °C for 900 s (figure 1(e)).

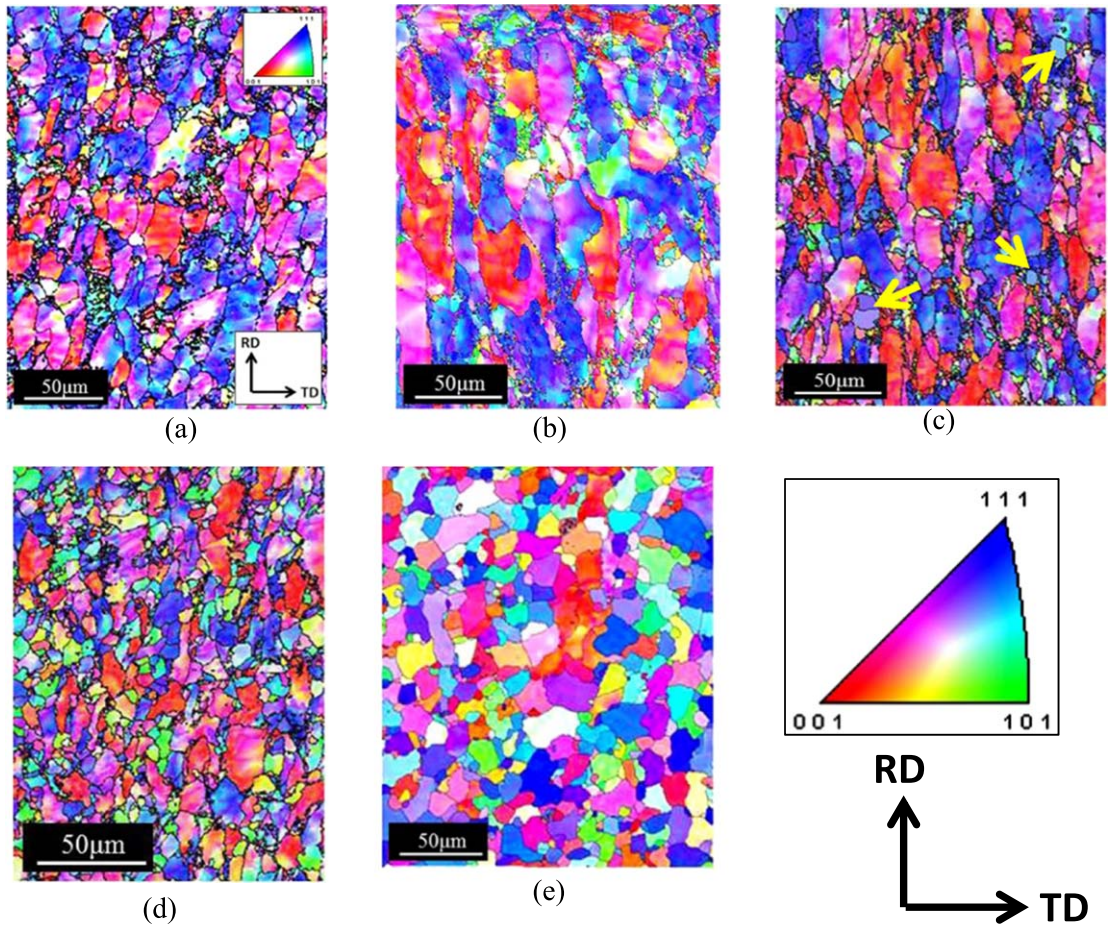

Figure 1. EBSD Orientation imaging maps after annealing at: (a) 400 °C/120 00 s (b) 520 °C/120 00 s (c) 580 °C/300 s (d) 640 °C/300 s and (e) 640 °C/900 s. Different colors in the maps correspond to varying crystallographic directions assigned to red ⟨001⟩, blue ⟨111⟩ and green ⟨101⟩.

The grain boundary characteristics and its misorientation distributions are explained in figures 2 and 3, respectively. The grain boundary misorientation map of low temperature (400 °C) annealed sample (figure 2(a)) explains the increasing of low angle (2–5°) grain boundary (LAB) fractions within the deformed grains. Upon annealing at 520 °C, the LAB fraction is lesser (figure 3), due to the subgrain structure formation within the deformed grains at this recovery stage (figure 2(b)). Further annealing at 580 °C leads to a decrease of LAB fractions and a little increase of high angle boundaries (HAB) for strain free grains (figure 2(c)). A similar result is also observed by Chao Fang *et al* for cold rolled HSLA steels [32]. They have noted that recrystallization begins and these low angle boundaries succeeded by high angle boundaries with increasing annealing temperature. The partial and completion of recrystallization at 640 °C for 300 and 900 s (figure 2(d) and (e)) cause the lowering of LAB (2–5° and 5–15° angle) and increasing of HAB fraction. The change from low to high angle boundaries also signifies the loss of stored energy with the progress of recrystallization.

The Kernal Average Misorientation (KAM) map is a method related to the significant lattice distortion on the point-to-point measurement, with the lattice orientation inside a grain [33]. In this study, the color green is committed to high KAM values and related to lattice defects, while the color blue grain shows the area of low KAM for stress-free region. At low annealing temperature (400 °C), high stored energy in deformed grain structure is revealed by the predominant green color of KAM map, indicating a sound signature of distorted accumulating stored energy with a KAM misorientation of 1°(figure 4(a)). The stored energy becomes marginal relief within each deformed grains at this annealing temperature (520 °C), which implies the occurrence of recovery in the form of substructure evolution (figure 4(b)). The present results are consistent with the literature reported by Zhang *et al* for 9Cr-1Mo deformed steel [34]. They have explained that the material first recovers and coarsens during annealing, which induces softening and reducing in stored energy. Figure 4(c) shows the strain free grains (blue color) of lesser lattice distortion at an average KAM value to nearly about 0.65° after intermediate annealing at 580 °C. Upon progress of annealing, the recrystallization causes deformed region and softened the material, corresponding to the lower KAM value owing to diminution in stored energy (figure 5). The increasing blue colored region for partially recrystallized sample (at 640 °C for 300 s) indicates the

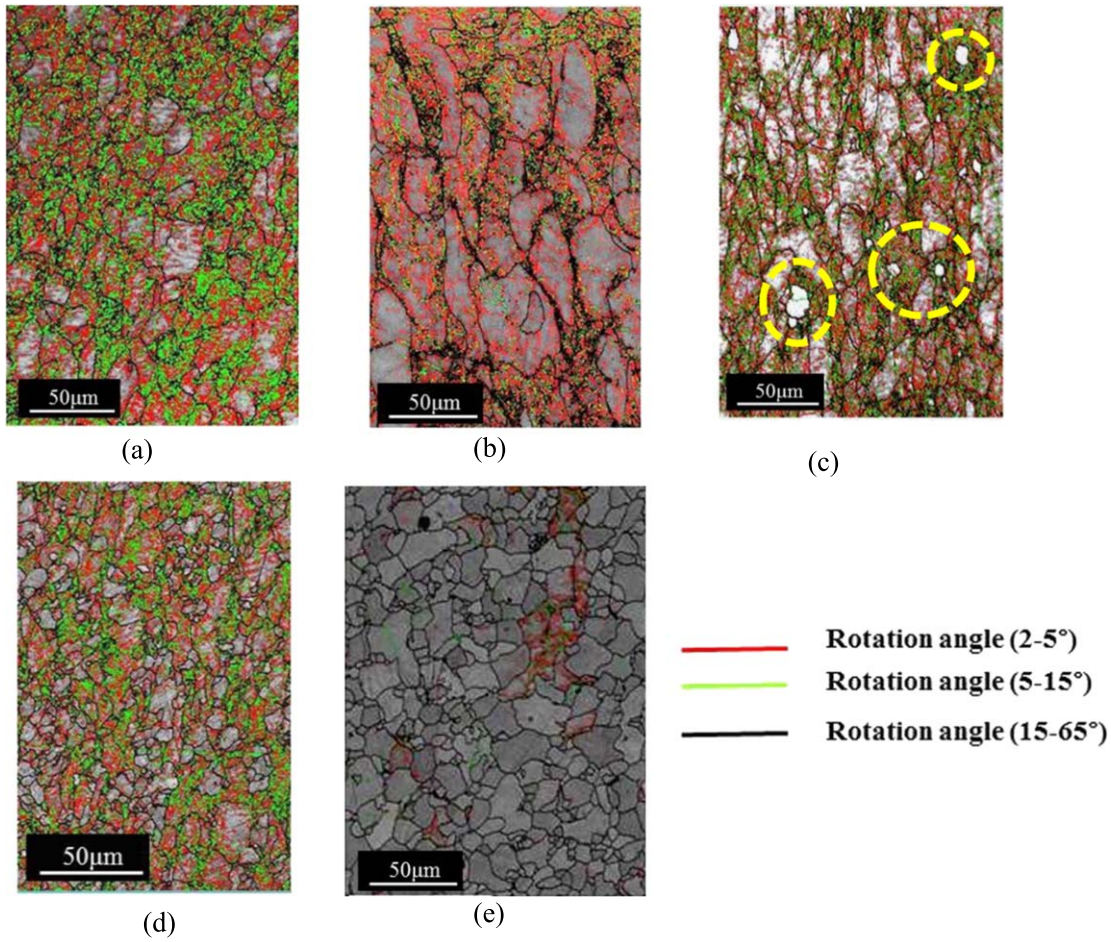

Figure 2. Misorientation grain boundary map of annealed samples for conditions of (a) 400 °C/120 00 s (b) 520 °C/120 00 s (c) 580 °C/3 00 s (d) 640 °C/3 00 s and (e) 640 °C/9 00 s, in which red and green colors display low angle boundary (<15°) and black line high angle boundary (>15°).

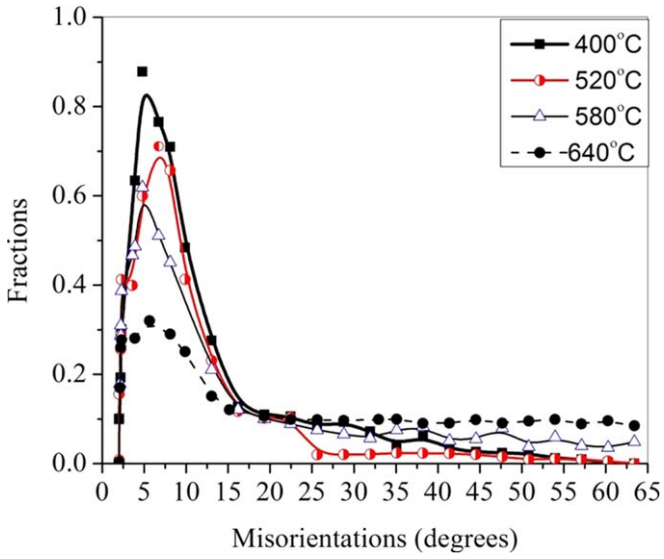

Figure 3. Variation of grain boundary misorientation distribution during annealing of ultra low carbon steel at different temperatures.

reductions of stored energy with an average KAM value of 0.62° (figures 4(d) and 5). The completion of recrystallization (at 640 °C for 900 s) represents the equiaxed ferrite grain (blue color), resulting in the lower orientation spread inside the grain (figure 5) with an average KAM value of 0.56° (figure 4(e)).

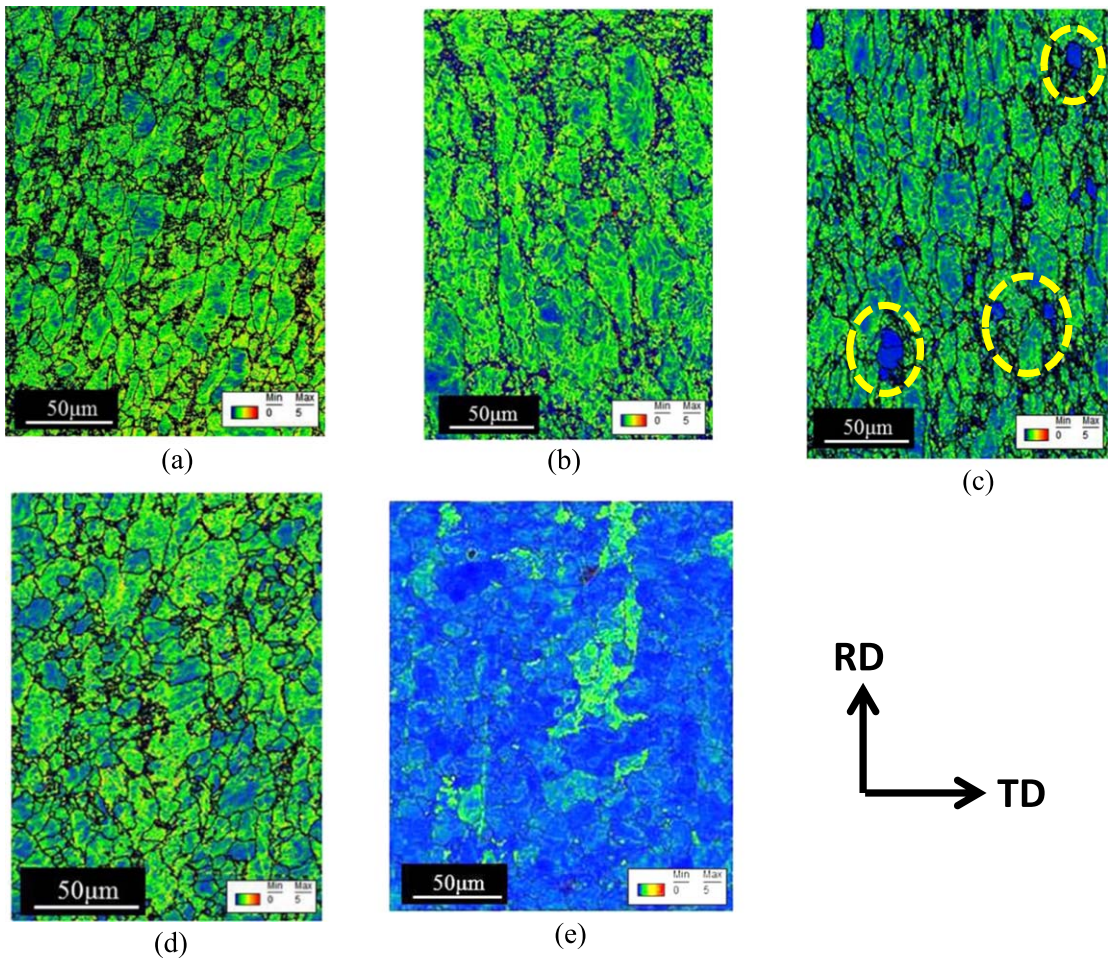

Figure 4. Kernel average misorientation map of annealed samples for (a) 400 °C/120 00 s (b) 520 °C/120 00 s (c) 580 °C/3 00 s (d) 640 °C/3 00 s and (e) 640 °C/9 00 s.

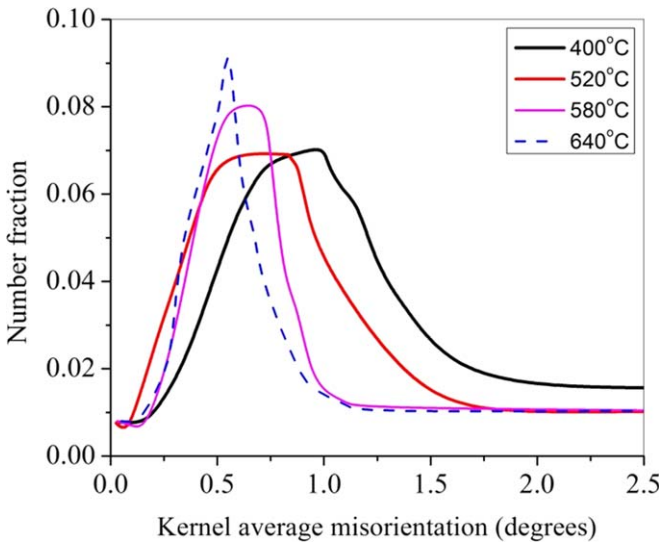

Figure 5. Distribution of Kernel average misorientation (KAM) for annealed ultra low carbon steel at different temperature.

3.2. Recovery and recrystallization kinetics

The recovery and recrystallization kinetics are determined by isothermally annealed samples at temperature of 350, 400, 520, 550, 580 and 640 °C. Several literatures have been reported for different models on the basis of

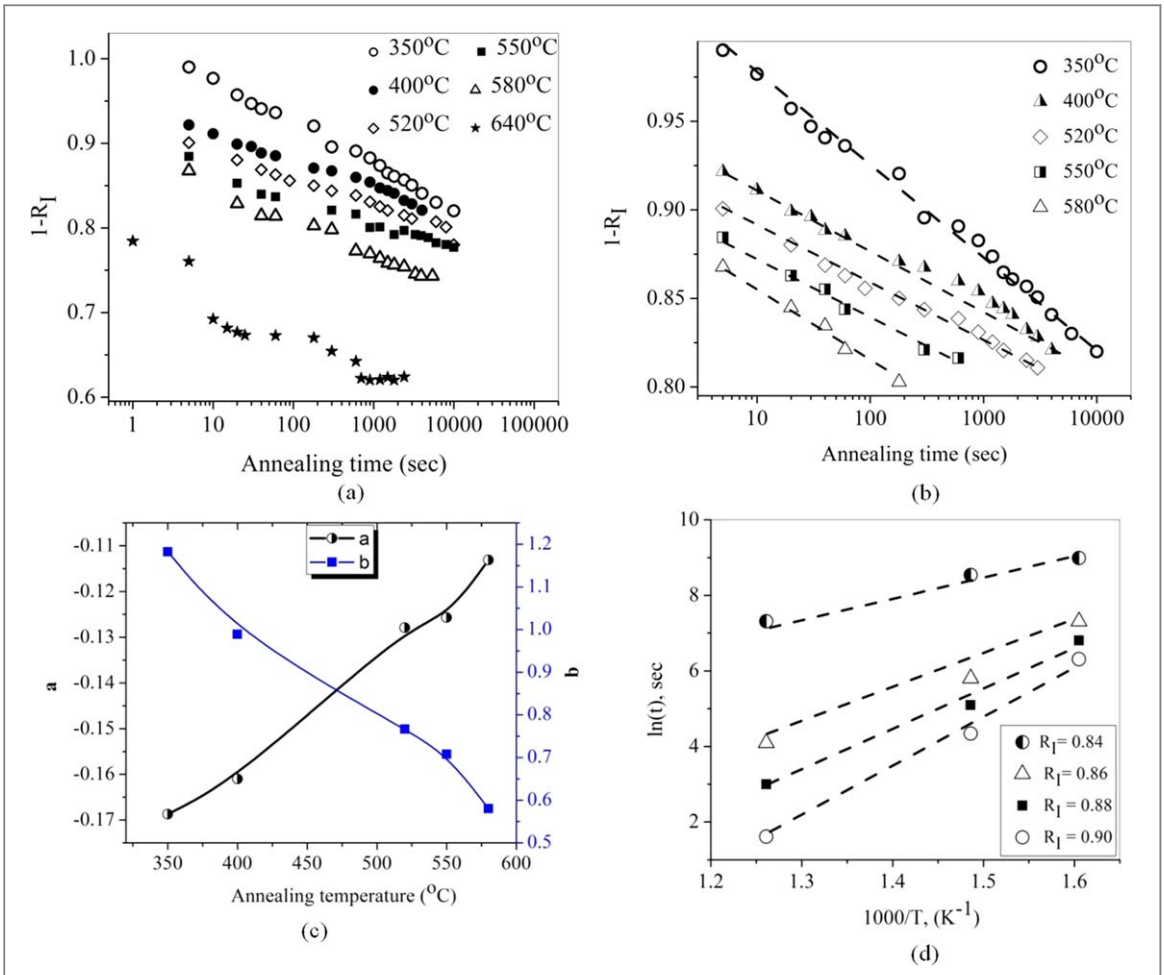

Figure 6. Explanation of recovery kinetics for ultra low carbon steel with evolution of residual strain (1-R_I) fraction as a function of annealing time at (a) different temperatures and (b) some specific temperatures for recovery region, (c) temperature dependence of constant parameters b and a, (c) logarithm of annealing time versus inverse absolute temperature at constant values of (1-R_I) fraction.

mechanical and magnetic parameters [35, 36]. Therefore, magnetic and mechanical softening due to decrease of coercivity and hardness are considered for recovery and recrystallization kinetics, respectively.

3.2.1. Recovery kinetics through magnetic softening

The magnetic coercivity is an extrinsic property of steel, relating to the crystal defects like dislocations. The cold rolled steel consists of elongated grain with high dislocation density which acts as the pinning sites against magnetic domain wall movement, and it results in an increase of coercivity (H_c) in cold deformed conditions [37]. Since the recovery relates to the rearrangement and annihilation of dislocations and the coercivity is linearly proportional to dislocation density ($Hc \propto \sqrt{\rho}$), the coercivity change during annealing is well established to explain the recovery kinetics of low carbon steel [35]. Accordingly, the recovery fraction (R_I) is derived from coercivity change of recovered structure relative to cold deformed steel coercivity and explained as follows,

$$R_I = \frac{H_{c,def} - H_{c,t}}{H_{c,def}} \quad (1)$$

where $H_{c,t}$, $H_{c,def}$ are coercivity for annealed and cold rolled sample, respectively.

The fraction of residual strain (1-R_I), which is equivalent to coercive field ratio ($\frac{H_{c,t}}{H_{c,def}}$), describes the recovery state of annealed steel as a function of annealing time (figure 6(a)). At low temperature ranges (350–520 °C), the coercivity value decreases linearly with the increase of annealing time, signifying the enhancement of magnetic softness in material at this recovery stage [7, 17]. It is attributed to the reductions in dislocation density and the resultant sub grain structure formation. At 550 and 580 °C, the initial shallow decrease of coercivity is followed by a sudden drop at annealing times of 900 and 300 s, and the strain free grain causes the coercivity saturation at 7500 and 5400 s, respectively [15]. At high annealing temperature (640 °C), the coercivity decreases during first 10 s, and it becomes stagnant between 15 to 180 s, representing the existence of stable dislocation structure and

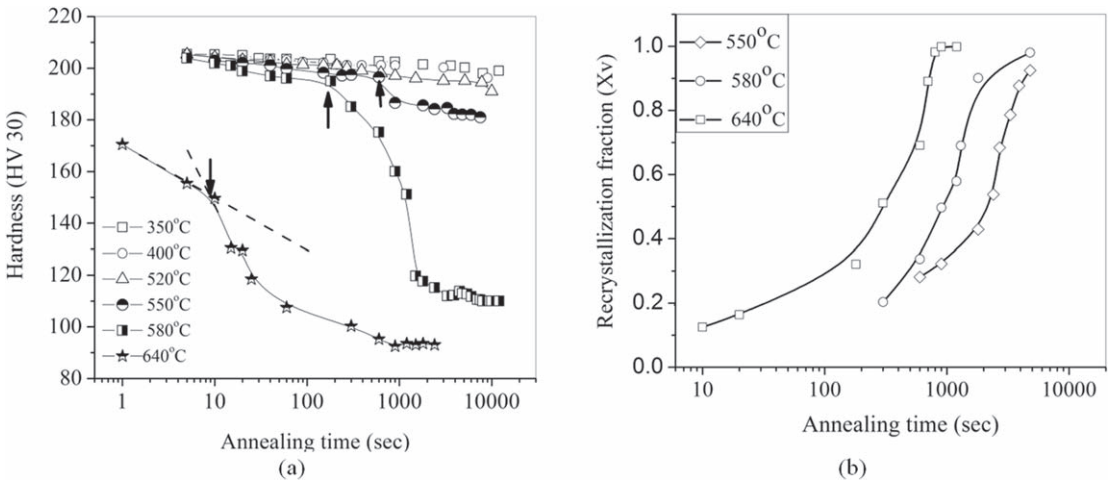

Figure 7. (a) Hardness variation as a function of annealing time (b) Softening recrystallization fraction (X_v) as a function of annealing time for cold rolled ultra low carbon steel (arrow explaining incubation time indicated by dotted lines at changing curve direction).

the development of strain free grains in the deformed material. Progress in annealing time at t > 180 s attends to a gradual fall of coercivity due to the increased of recrystallization rate with the number of strain free grains as the significance of partial recrystallization, described in figure 1(d). The continual increase of strain frees grains with the expense of deformed region results in the completion of recrystallization at 900 s, indicating by the coercivity stagnancy.

For recovery kinetic study, the residual strain (1-R_I) fraction is re-plotted for annealing at low temperature (350, 400, 520 °C) and an initial time of 300 and 240 s for 550, 580 °C, respectively, as shown in figure 6(b). The (1-R_I) values at different annealing temperatures are explained by the logarithmic relationship [4], as follows,

$$1 - R_I = b - a \ln t \tag{2}$$

where a and b are constants for each annealing temperature.

The a and b constants are determined by the least square fitting of (1-R_I) values in figure 6(b), and these are varied as a function of annealing temperature (figure 6(c)). It is found that the effect of annealing temperature on a and b parameters are a reverse trend. Mukunthan *et al* also reported a similar type of behavior for cold rolled steel by x-ray peak intensity measurements. They have stated that this type of dependence are mainly associated to the reduction of dislocation density owing to recovery [4].

As per Arrhenius relationship, the recovery rate can be explained as follows,

$$\text{Rate} = \frac{1}{t} = -A \exp\left(-\frac{Q}{RT}\right) \tag{3}$$

where R is the universal gas constant in kJ mol^{-1}, Q is the activation energy (kJ mol^{-1}) for recovery and T is the absolute temperature. Moreover, the instantaneous rate of recovery is obtained by the line intercept method for each constant (1-R_I) fractions of 0.9, 0.88, 0.86 and 0.84 in figure 6(b). The resultant annealing time and temperatures are represented in figure 6(d), corresponding to equation (3). Accordingly, the slopes of liner fitting lines are equivalent to activation energy (Q), described in table 2. With increasing recovery fraction (R_I) from 0.84 to 0.90, the activation energy increases from 41 to 113 kJ mol^{-1}. The lower activation energy at the initial of recovery is owing to high stored energy developed through high dislocation density at the deformation. The activation energy for Ti-Nb stabilized IF steel increases to 173–312 kJ mol^{-1} with the effect of excess solute Ti and Nb at the iron lattice or fine carbides and nitrides are accomplished of restraining the recovery process [4, 36]. Similarly, Alvarez *et al* reported that the activation energies of Cr-Mo pre-strained steel are 288.3 and 266.6 kJ mol^{-1} for 2.6 and 7 pct deformation, respectively [37]. According to their model, the activation energy in prestrain steel decreases with the consequence of higher driving force generation by high dislocation density and internal stress. The completion of recovery is followed by the generation of strain free grains with the increase of annealing time, increasing the mechanical softening.

3.2.2. Recrystallization kinetics through mechanical softening

Figure 7(a) represents the hardness variation for annealed ultra low carbon steels as a function of annealing time at different temperatures. The minimal hardness change at temperature 350–520 °C is owing to the occurrence of recovery by annihilation and rearrangement of dislocations. At 550 and 580 °C, the hardness variation is initially slow for recovery and then decreases abruptly at 900 and 300 s, due to the strain free grains nucleation in

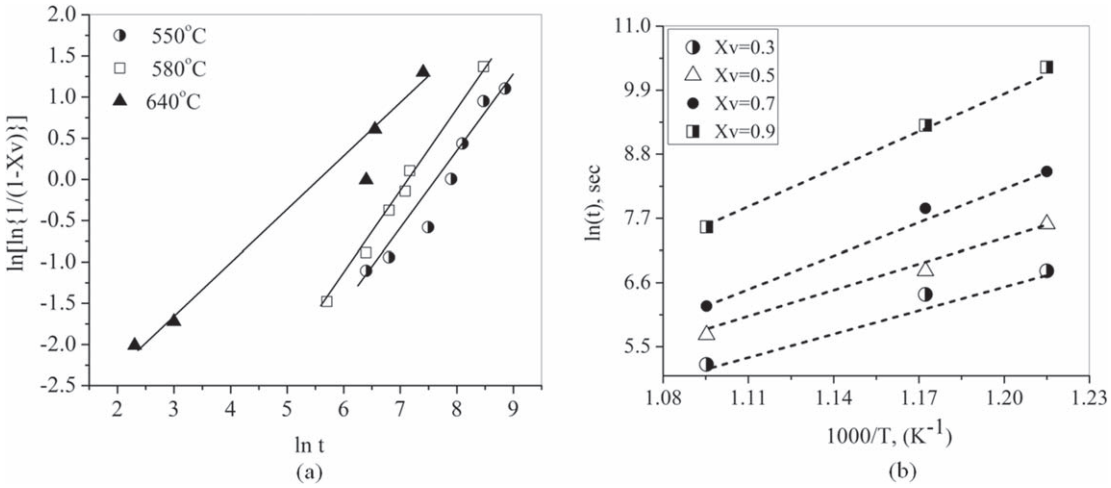

Figure 8. (a) Avrami plot of ln[ln{1/(1-Xv)}] versus ln(t) for cold rolled annealed samples at 550,580 and 640 °C and (b) Arrhenius plot of the kinetics functions ln(t) versus 1000/T(K^{-1}) for ultra low carbon steel.

Table 1. JMAK fitting parameters n and k.

Annealing temperature(°C)	n	k	R^2
550	1.05	0.053 71	0.91
580	1.15	0.034 32	0.94
640	1.22	0.0264	0.96

the deformed matrix (as observed in figure 1(c)). Other researchers have also reported the hardness variation of extra low carbon cold rolled steel takes place a small change during recovery and continuous drop upon progress of recrystallization [7]. At higher temperature (640 °C), the hardness drops at 10 s for nucleation of strain-free grain, and then gradually decreases with increasing annealing time, relating to more strain free grain formation (partially recrystallization as examined in figure 1(d)). The recrystallization completes at 640 °C for 900 s, and it is followed by a stagnancy of hardness with the increasing annealing time. This hardness change, which is also equivalent to recrystallization fraction (X_v) using an equation (4), and mechanical softening, has been found more promising to monitoring behavior of cold rolled steels [22].

$$Xv = \frac{(H_0 - H_t)}{(H_0 - H_{rex})} \tag{4}$$

where H_0, H_t, and H_{rex} are hardness of cold rolled, annealed one and fully recrystallized samples, respectively. Accordingly, the hardness measurement is deliberated for recrystallization kinetic study at high temperature (550, 580 and 640 °C), and the recrystallization fraction (X_v) is described as a function of annealing time (figure 7(b)). The incubation time for recrystallization start is 900 and 300 s for 550 and 580 °C temperatures, respectively. The recrystallization rate is obtained much faster at 640 °C than 550 and 580 °C. Accordingly, the recrystallization fraction at 640 °C corresponds to the recrystallization rate with an incubation time of 10 s, an increasing rate at linear region of 180-700 s, and finally a decreasing rate of 800–900 s.

In general, the recrystallization kinetics is related to thermally activated methods of nucleation and grain growth processes, defined by Johnson Mehl Avrami and Kolmogorov (JMAK) equation (5) [32] as follows,

$$X_v = 1 - \exp(-kt^n) \tag{5}$$

where X_v is recrystallization fraction at the time 't', k is a temperature dependent constant and 'n' is known as the Avrami or JMAK exponent. Figure 8(a) shows a nearly linear regression plot of ln(ln1/(1-Xv)) versus ln(t), and the slope and intercept are determined as 'n' and 'k', respectively (table 1). The value of JMAK exponents of 'n' increases, while the parameter 'k' decreases with the increasing annealing temperature. Several researches on JMAK model are available for different materials such as low carbon, aluminum and copper [38–40]. As per the theoretical assumption of JMAK model, the site saturation nucleation model predicts $n = 3$ while the constant nucleation rate model predicts $n = 4$. These theoretical values are on the basis of isotropical growth of grains in three dimensions until impingement [1]. The lowering of JMAK exponent occurs with the inhomogeneous distribution of nucleation site, anisotropic growth of nuclei and the varying growth rate by microstructural features [41]. The 'n' values in present investigation are found to below the theoretical values in an order of

Table 2. Activation energy (Q) of cold rolled ultra low carbon steel for recovery and recrystallization.

Activation energy for recovery		Activation energy for recrystallization	
Recovery fraction (R_1)	Q (kJ mol^{-1})	Recrystallization fraction	Q_{rex} (kJ mol^{-1})
0.84	41	0.30	114
0.86	76	0.50	130
0.88	91	0.70	162
0.90	113	0.90	190

1.05–1.22 with increasing temperatures of 550–640 °C, attributed to the inhomogeneous nuclei distribution which is also featured in figure 1(c). Marwan also reported low 'n' values of 1.39–1.98 for 20%–90% cold rolled steel [42]. They have explained the slow mechanism of initial recrystallization, which attributed to the occurrence of solute atoms in an iron lattice. Moreover, other researchers have reported the variation of 'n' values for high strength IF steel between 1.4 at 675 °C and 1.03 at 800 °C for unidirectional rolled samples, while 'n' varies between 0.83 at 675 °C and 2.6 at 800 °C for cross rolled samples [36]. The constant 'k' value decreases with, reflecting the temperature dependence for nucleation and growth rates [3]. Since JMAK model has no direct relation to any microstructural parameters (e.g. grain size), the complex process like recrystallization cannot be completely described by this model. Although the temperature dependence of recrystallization kinetics arises the Arrhenius-type relationship, and the apparent activation energy can be exposed in equation (6) as follows[3],

$$t_x \propto \exp\left(\frac{Q_{rex}}{RT}\right) \tag{6}$$

where 't_X' is the time required for progressing recrystallization process, Q_{rex} is the activation energy associated to the recrystallization, R is the universal gas constant and T is the temperature in kelvin.

The activation energy for recrystallization is calculated from the slope of linear plots of ln(t) versus 1000/T (figure 8(b)) and explained in table 2. The increasing of recrystallization fraction decreases driving force and/or mobility of grain boundaries, resulting in the rise of activation energy. The values of the activation energy estimated for recrystallization (Q_{rex}) increases from 114–190 kJ mol^{-1} with recrystallization fraction increasing from 0.30 to 0.90. Khatirkar *et al* reported the activation energy of unidirectional cold rolled (80%) interstitial free high strength (IF-HS) steel is 216 kJ mol^{-1} for annealing temperatures of 675 and 800 °C [36]. The activation energy of low carbon (0.025 and 0.155 wt%) plastically strained steels is explained between 276.12–287.56 kJ mol^{-1} [43]. The activation energy increases with carbon content owing to the glide and interactions of dislocations for higher carbon content at high Z (Zener Hollomon parameter) values. In addition, the higher activation energy is also reported for cold rolled Ti-Nb stabilized IF steels (502 kJ mol^{-1}), mainly effect owing to restraining by fine precipitates solute atoms in the solid iron lattice [4]. The typical grain boundary movements during recrystallization are mostly controlled by thermally activated transport process. The change in activation energy during recrystallization is mainly associated to the atomistic mechanism responsible for grain boundary migration.

4. Conclusions

The kinetics of recovery and recrystallization behavior of cold rolled ultra low carbon steel are studied at the isothermal annealing temperature range between 350–640 °C. The conclusions of this investigation are drawn as follows:

1. Upon progress of annealing, the orientation of subgrain is found along ⟨001⟩ and ⟨111⟩//ND at 520 °C, while the strain free grains are oriented with ⟨111⟩ orientation at 580 °C. The completely recrystallized ferrite grains with an average size of 14 μm are found in the sample annealed at 640 °C for 900 s.
2. The coercivity ratio, evaluated from annealed to cold rolled steel, is equivalent to residual strain (1-R_I) for kinetics study. The activation energy for recovery increases from 41 to 113 kJ mol^{-1} with increasing R_I from 0.84 to 0.90.
3. The recrystallization fraction, obtained from mechanical softening, explains the JMAK exponent (n) variation in an order of 1.05–1.22 with recrystallization temperatures of 550–640 °C.

4. The recrystallization completion occurs at 640 °C for 900 s. The recrystallization kinetics is also considered by the Arrhenius-type relationship, and the activation energy varies from (114–190 kJ mol^{-1}) as a function of annealing time.

5. The release of stored energy during recovery and recrystallization follows the progress of softening fractions with increasing high angle grain boundaries and lowering KAM value (<1°).

Acknowledgments

The authors would like to express their sincere thanks to Director, National Metallurgical Laboratory, Jamshedpur, for his permission to use the infrastructural equipment and to publish the paper. The authors are also thankful to Dr Subrata Mukherjee, Tata steel R&D Centre Jamshedpur, India, for his help to get the EBSD characterization used in this research work. The financial assistance to one of the authors (Siuli Dutta) by Council of Scientific and Industrial Research, India, is gratefully acknowledged.

ORCID iDs

Ashis K Panda https://orcid.org/0000-0002-1199-2100
Rajat K Roy https://orcid.org/0000-0002-3978-0054

References

[1] Humphreys F J and Hatherly M 1996 *Recrystallization and Related Annealing Phenomena.* (Oxford, UK: Pergamon Press) pp 127
[2] Alvarez M A, Marchena M and Perez T 2008 Recovery kinetics of cold—deformed Cr–Mo steels *Metall. Mater. Trans* A **39** 3283–90
[3] Farzadi A 2015 Modeling of isothermal recovery and recrystallization kinetics by means of hardness measurements *Mat. Wiss.* **46** 12
[4] Mukunthan K and Hawbolt E B 1996 Modeling recovery and recrystallization kinetics in cold rolled Ti–Nb stabilized interstitial-free steel metall *Mater. Trans.* A **27A** 3410–22
[5] Husain Z 1993 The assessment of recrystallization in low carbon low alloy steel using alternating current potential drop (ACPD) measurements *Mater. Sci. Forum* **113–115** 667–72
[6] Torres C E, Rodriguez, Sanchez F H, Gonzalez A, Actis F and Herrera R 2002 Study of kinetics of the Recrystallization of cold rolled low carbon steel *Metall. Mater. Trans.* A **33A** 25–33
[7] Martinez-de-Guerenu A, Arizti F, Fuentes M and Gutierrez I 2004 Recovery during annealing in a cold rolled low carbon steel part I: kinetics and microstructural characterization *Acta Mater.* **52** 3657–64
[8] Gupta S k, Raja R A, Vashista M and Yusufzai M 2019 Hysteresis loop analysis of gas metal arc welded ferritic stainless steel plate *Mater. Res. Express.* **6** 096110
[9] Roy R K, Premkumar M, Panda A K and Mitra A 2018 Utilization of electromagnetic sensor for structural characterization of steels during processing and in-service components', in industry interactive innovations in science, engineering and technology *Notes in Networks and Systems* **11** 247–54
[10] Mitra A, Mohapatra J N, Swaminathan J, Ghosh M, Panda A K and Ghosh R N 2007 Magnetic evaluation of creep in modified 9Cr–1Mo steel *Scripta Mater* **57** 813–6
[11] Moorthy V, Vaidyanathan S, Baldev R, Jayakumar T and Kashyap B P 2000 Insight into the microstructural characterization of ferrite steels using micromagnetic parameters *Metall. Mater. Trans.* A **31A** 1053–64
[12] Kumar H, Mohapatra J N, Roy R K, Josephus R J and Mitra A 2009 Evaluation of tempering behavior in modified 9Cr–1Mo steel by magnetic non-destructive techniques *J. Mater. Process Tech* **210** 669–74
[13] Altpeter I, Tschuncky R and Szielasko K 2016 Electromagnetic techniques for materials characterization *Materials Characterization Using Nondestructive Evaluation (NDE) Methods* ed Gerhard Hübschen *et al* (United Kingdom: Woodhead Publishing) pp 225–262
[14] Chen H, Xie S, Chen Z, Takagi T, Uchimoto T and Yoshihara K 2014 Quantitative nondestructive evaluation of plastic deformation in carbon steel based on electromagnetic methods *Mater. Trans.* **55** 1806–15
[15] Oyarzabal M, Gurruchaga K, Martinez-de-Guerenu A and Gutierrez I 2007 Sensitivity of conventional and non-destructive characterization techniques to recovery and recrystallization *ISIJ Int.* **47** 1458–64
[16] Zhou L, Liu J, Hao X J, Strangwood M, Peyton A J and Davis C L 2014 Quantification of the phase fraction in steel using an electromagnetic sensor *NDT. Int.* **67** 31–5
[17] Oyarzabal M, Martinez-de-Guerenu A and Gutierrez I 2008 Effect of stored energy and recovery on the overall recrystallization kinetics of a cold rolled low carbon steel *Mater. Sci. Eng.* A **485** 200–9
[18] Roy R K, Dutta S, Panda A K, Rajinikanth V, Das S K, Mitra A, Strangwood M and Davis C L 2018 Assessment of recovery and recrystallisation behaviors of cold rolled IF steel through nondestructive electromagnetic characterization *Phil. Mag.* **98** 1933–44
[19] Kikuchi H, Ito F, Murakami T and Takekawa K 2015 Relation between magnetic properties and hardness and its effect on recovery and recrystallization in cold-rolled steel *IEEE Trans. Mag.* **45** 2744–7
[20] Martinez-de-Guerenu A, Oyarzabal M, Arizti F and Gutierrez I 2005 Application of coercive field measurements to the evaluations of recovery and recrystallization in cold rolled interstitial (IF) steel *Mater. Sci. Forum.* **500–501** 647–54
[21] Martinez-de-Guerenu A, Arizti F and Gutierrez I 2004 Determination of the recovery kinetics during the annealing of cold rolled low carbon steels *Mater. Sci. Forum.* **467–470** 141–6
[22] Dutta S, Rajinikanth V, Panda A K, Mitra A, Chatterjee S and Roy R K 2019 Effect of annealing treatment on mechanical and magnetic softening behaviors of cold rolled interstitial-free steel *J. Mater. Eng. Perform.* **28** 2228–36
[23] Martinez-de-Guerenu A, Badiola D J and Gutierrez I 2017 Assessing the recovery and recrystallization kinetics of cold rolled microalloyed steel through coercive field measurements *Mater. Sci. Eng.* A **691** 42–50
[24] Jonas J J 1980 Kinetics of recovery and recrystallization in polycrystalline copper *Acta. Mater.* **28** 729–43

[25] Yashin V, Aryshenskii E, Hirsch J, Konovalov S and Latushkin I 2019 Study of recrystallization kinetics in AA5182 aluminium alloy after deformation of the as-cast structure *Mater. Res Express* **6** 066552
[26] Jonas J J, Quelennec X, Jiang L and Martin E T 2009 The Avrami kinetics of dynamic recrystallization *Acta. Mater.* **57** 2748–56
[27] Vandermeer R A and Hansen N 2008 Recovery kinetics of nanostructured aluminum: model and experiment *Acta. Mater.* **56** 5719–27
[28] Thomas I, Zaefferer S and Rabbe D 2003 High resolution EBSD investigation of deformed and partially recrystallized IF steel *Adv. Eng. Mater.* **5** 566–70
[29] Eskandari M, Mohtadi-Bonab M A and Szpunar J A 2016 Evolution of the microstructure and texture of X70 pipeline steel during cold-rolling and annealing treatments *Mater. Design.* **90** 618–27
[30] Roy R K, Panda A K and Mitra A 2012 An electromagnetic sensing device for microstructural Phase determination of steels through non-destructive evaluation *Proc. of 6th Int. Conf. on Sensing Technology* (IEEE Xplore) pp 226–229
[31] Humphreys F J and Hatherly M 2004 *Recrystallization and Related Annealing Phenomena* (Oxford: Elsevier) 2nd edn (https://doi.org/10.1016/B978-0-08-044164-1.X5000-2)
[32] Fang C, Garcia C, Choi S and Deardo A 2015 A study of the batch annealing of cold-rolled HSLA steels containing niobium or titanium *Metall. Mater. Trans.* A **46A** 3635–45
[33] Brewer L N, Field D P, Merriman C C, Kumar B L, Schwartz A J, Adams M and Field D 2009 *Electron Backscatter Diffraction in Mater. Sci.* (New york, NY: Springer) 1st edn (https://doi.org/10.1007/978-1-4757-3205-4)
[34] Zhang Z, Zhang Y, Mishin O, Tao N, Pantleon W and Jensen D 2016 Microstructural analysis of orientation-dependent recovery and recrystallization in a modified 9Cr-1Mo steel deformed by compression at a high strain rate *Metall. Mater. Trans.* A **47A** 4682–92
[35] Martinez-de-Guerenu A, Arizti F and Gutierrez I 2004 Recovery during annealing in a cold rolled low carbon steel part II: Modelling the kinetics *Acta Mater.* **52** 3665–70
[36] Surthi K K, Khatirkar R K and Sapate S G 2013 Effect of mode of rolling on recrystallization kinetics and microstructure evolution in interstitial free high strength steel sheet *ISIJ Int.* **53** 356–64
[37] Alvarez M A V, Marchena M and Perez T 2008 Recovery kinetics of cold-deformed Cr–Mo steels *Metall. Mater. Trans.* A **39A** 3283–90
[38] Leslie W C, Michalak J T and Aul F W 1963 *The Annealing of Cold- Worked iron, in iron and its Dilute Solid Solutions* ed C W Spencer and F E Werner (New York, NY: Interscience) pp 119–212
[39] Gordon P and Vandermeer R A 1962 Mechanism of boundary migration in recrystallization *Trans. Metall. Soc.* **224** 917–28
[40] Rosen A, Burton M S and Smith G V 1964 Recrystallization of high-purity iron *Trans. Met. Soc. AIME,* **230** 205–15
[41] Verlinden B, Driver J, Samajdar I and Doherty R D 2007 Thermo-Mechanical Processing of Metallic Materials *Pergamon Materials Series* vol 11 ed Bert Verlinden *et al* (USA: Elsevier Science) pp 1–528
[42] Almojil M A 2010 Deformation and recrystallisation in low carbon steels *Ph. D Thesis* University of Manchester, UK
[43] Hernandez C A and Mancilla J E 2003 Effect of low carbon contents on the activation energy for plastic deformation upon steels *Mater. Sci. Forum.* **426–432** 1331–6